Supporting Information for "A Lagrangian perspective on tropical anvil cloud lifecycle in present and future climate"

Blaž Gasparini[1], Philip J. Rasch[2], Dennis L. Hartmann[1], Casey J. Wall[3], Marina Dütsch[1]

[1]University of Washington, Seattle, Washington, USA

[2]Pacific Northwest National Laboratory, Richland, Washington, USA

[3]Scripps Institution of Oceanography, University of California San Diego, USA

Contents of this file

1. Text S1 to S3
2. Figure S1 to S4
3. Table S1

Additional Supporting Information (Files uploaded separately)

1. Captions for Movie S1

Introduction

The supporting material includes 4 additional figures that either show more support of the study's main findings (Fig. S1, S2, S4, Table S1) or reveal additional information that help interpret some of the study's results (Fig. S3).

Text S1. The decay of anvil cloud fraction is not significantly biased by our decision to consider only trajectories not encountering any significant ice detrainment tendency after the initial 4 hours of the evolution (Fig. S1). Interestingly, the lifetime slightly decreases with the inclusion of such trajectories, most likely due to stronger resolved vertical velocities near regions of active convection, which loft the trajectories, often ending above the cloud top.

The standard set of trajectories uses a minimum IWC limit of 0.1 mg kg^{-1} for the determination of a cloud. The lifetime decreases by about 2.5 hours when using an order of magnitude larger ice mixing ratio limit in the definition of a cloud lifetime, similar to that used by Mace, Deng, Soden, and Zipser (2006), while a lower ice limit would not change the cloud lifetime (Fig. S2a). The lifetime was also found to be sensitive to the minimum cloud fraction allowed for calling an air parcel cloudy. The lifetime increases by about 2.5 hours when using a limit of 1% cloud fraction instead of the default value of 10%. On the other hand, the lifetime decreases by 2 hours when increasing the limit from 10% to 30% (Fig. S2b).

Text S2. We provide additional discussion in support of the cloud feedback calculation presented in Fig. 12. The discussion is supported by the cloud fraction histograms based on the instantaneous cloud fraction values computed by the ISCCP cloud simulator (Fig. S3), which are used in the cloud feedback calculations. The model-derived cloud fraction shows a clear maximum above 310 hPa for all COD bins (Fig. S3a). The high cloud fraction computed by the ISCCP simulator shifts to higher pressure levels (Fig. S3d) and

shows a small cloud fraction increase in warmer climate (Fig. S3e,f). In contrast, the low level cloud fraction decreases with warming in all COD bins (Fig. S3d-f).

Note that the cloud fraction values based on ISCCP simulator can differ from the model simulated ones (Pincus et al., 2012). For example, ISCCP simulator indicates an increase in high cloudiness for the clim4K with respect to the climREF simulation, whereas E3SM alone indicates a decrease (Fig 11a). The ISCCP estimate is used in the cloud feedback calculation and results in the positive LW and negative SW high cloud amount feedback (see Fig. 12b) as expected in the case of the high cloud fraction increase. When considering the amount feedback for all clouds (Fig. 12a), the LW and SW feedback components change sign, with the LW amount feedback being negative and the SW feedback being positive. This is typical of a decrease in high cloud fraction, in the apparent contrast to the results of Fig. 12b and is an artifact of the cloud amount feedback calculation, which assumes a fixed cloud distribution in pressure and optical depth levels. In particular, the proportion of high vs. low clouds has to remain constant, which is in violation of the simulated cloud differences, leading to a biased total cloud amount feedback (for a more complete discussion please refer to Zelinka, Klein, and Hartmann (2012) and the supplementary material of Zelinka, Zhou, and Klein (2016)).

High clouds have a strong effect on the OLR and are therefore expected to dominate the changes in altitude feedbacks, with only a small contribution from low clouds. It is therefore surprising to see the high cloud altitude feedback resulting in only about 50% of the total altitude cloud feedback (confront Figs. 12b and 12a). However, as a dif-

ference from the amount feedback, the calculation of cloud altitude feedback considers the non-proportionate change in cloud fraction, i.e. the residual between the actual and proportionate cloud fraction change. The residual (and therefore the altitude feedback) is large when considering clouds of all altitudes, due to the differences in the proportionality of high vs. low clouds in the warmer simulation (high cloud fraction increases, low cloud fraction decreases). The difference between the actual and proportionate cloud fraction changes decreases when considering high clouds only, leading to a smaller altitude feedback (Fig. 12b).

Finally, the optical depth feedback is large and negative for high clouds, which is consistent with the observed shift of the high cloud distribution in Fig. S3c towards larger COD bins. In contrary, low clouds exhibit no large optical depth shifts. The total optical depth cloud feedback is therefore as expected dominated by the high cloud feedback component, caused by an increase in ice water content (Fig. 11g).

Text S3. The values of both SW and LW CRE averaged along detraining trajectories are larger when, as a difference from the main manuscript (Table 3), the trajectories experiencing detrainment after the first 4 hours of the evolution are included in the statistical analysis (Table S1). This is an expected result: the additional detrainment leads to direct injections of ice and vapor, which increase the thick and intermediately thick anvil cloud fraction. While the impact of detrainment events encountered by trajectories after the first 4 hours of the cloud evolution is not negligible, these late detrainment events are not strong enough to change the qualitative picture of anvil cloud evolution including the relative importance of source and sink processes, ice cloud properties, or radiative effects.

Movie S1. 2-week long animation of the OLR simulated by the REF simulation (in filled contours). Tracked MCS are delineated by red contour lines. The plotted trajectories are colored based on their ice water content. Trajectories are plotted only as long as their ice water content is larger than 0.1 mg kg^{-1}. Each trajectory segment gradually fades through time, becoming fully transparent 12 hours after the trajectory overpass. The starting locations of trajectories are represented by red crosses.

References

Mace, G. G., Deng, M., Soden, B., & Zipser, E. (2006). Association of Tropical Cirrus in the 10–15-km Layer with Deep Convective Sources: An Observational Study Combining Millimeter Radar Data and Satellite-Derived Trajectories. *J. Atmos. Sci.*, *63*(2), 480–503. doi: 10.1175/JAS3627.1

Pincus, R., Platnick, S., Ackerman, S. A., Hemler, R. S., & Patrick Hofmann, R. J. (2012). Reconciling simulated and observed views of clouds: MODIS, ISCCP, and the limits of instrument simulators. *J. Clim.*, *25*(13), 4699–4720. doi: 10.1175/JCLI-D-11-00267.1

Zelinka, M. D., Klein, S. A., & Hartmann, D. L. (2012). Computing and Partitioning Cloud Feedbacks Using Cloud Property Histograms . Part II : Attribution to Changes in Cloud Amount , Altitude , and Optical Depth. *J. Clim.*, *25*, 3736–3754. doi: 10.1175/JCLI-D-11-00249.1

Zelinka, M. D., Zhou, C., & Klein, S. A. (2016). Insights from a Refined Decomposition of Cloud Feedbacks. *Geophys. Res. Lett.*, *43*. doi: 10.1002/2016GL069917

Table S1. Mean changes in cloud radiative effects (CRE) during 24 h along all computed trajectories. This includes also trajectories that experienced significant detrainment tendencies after the first 4 hours of the evolution, which were excluded from the analysis considered in the main part of the manuscript.

	REF	**4K-REF**
LW CRE [W m^{-2}]	87.2	8.1
SW CRE [W m^{-2}]	-94.5	-11.0
NET CRE [W m^{-2}]	-7.4	-2.9
NET feedback [W m^{-2} K^{-1}]	/	0.3

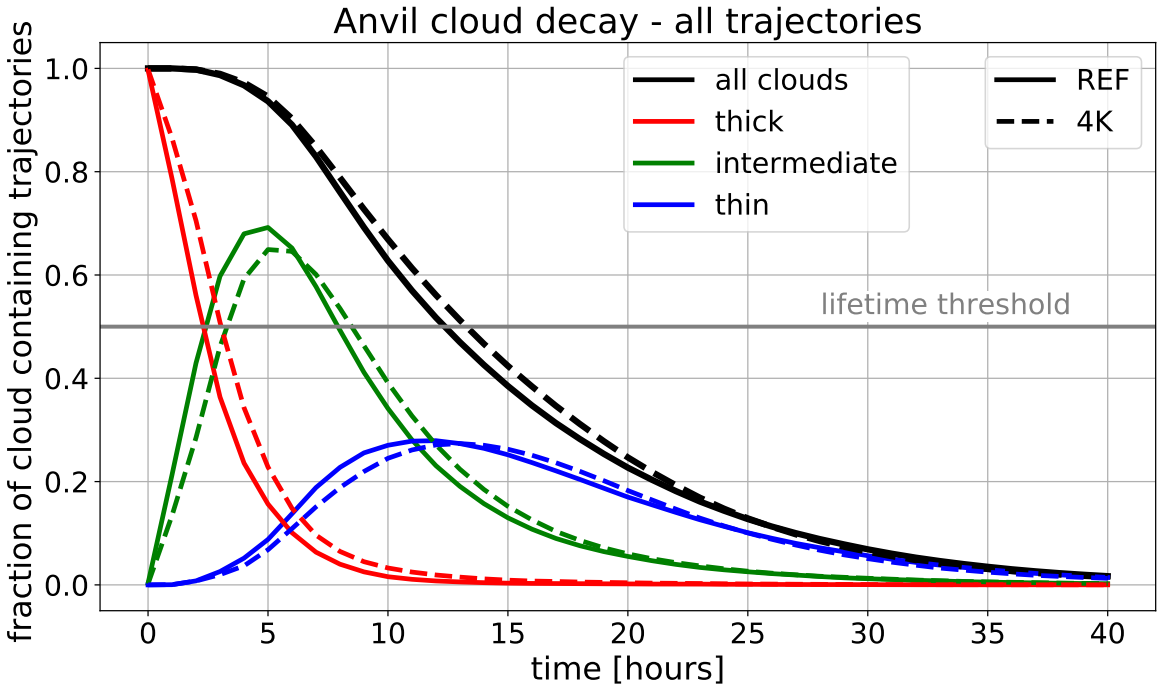

Figure S1. As Fig. 6 but with all trajectories considered (i.e. including those affected by subsequent detrainment of ice after hour 4 of the evolution).

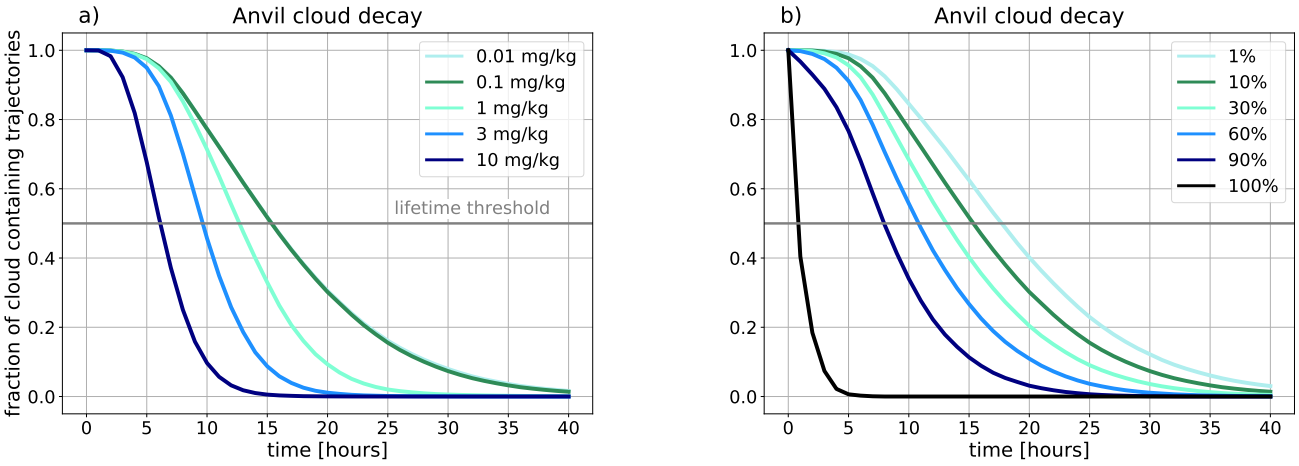

Figure S2. Sensitivity tests of anvil cloud decay when using different in-cloud IWC limits for cloud definition and a constant minimum cloud fraction limit of 10% (a). Sensitivity tests with different minimum cloud fraction limits considered in the definition of anvil cloud and a constant minimum in-cloud IWC limit of 0.1 mg kg^{-1} (b).

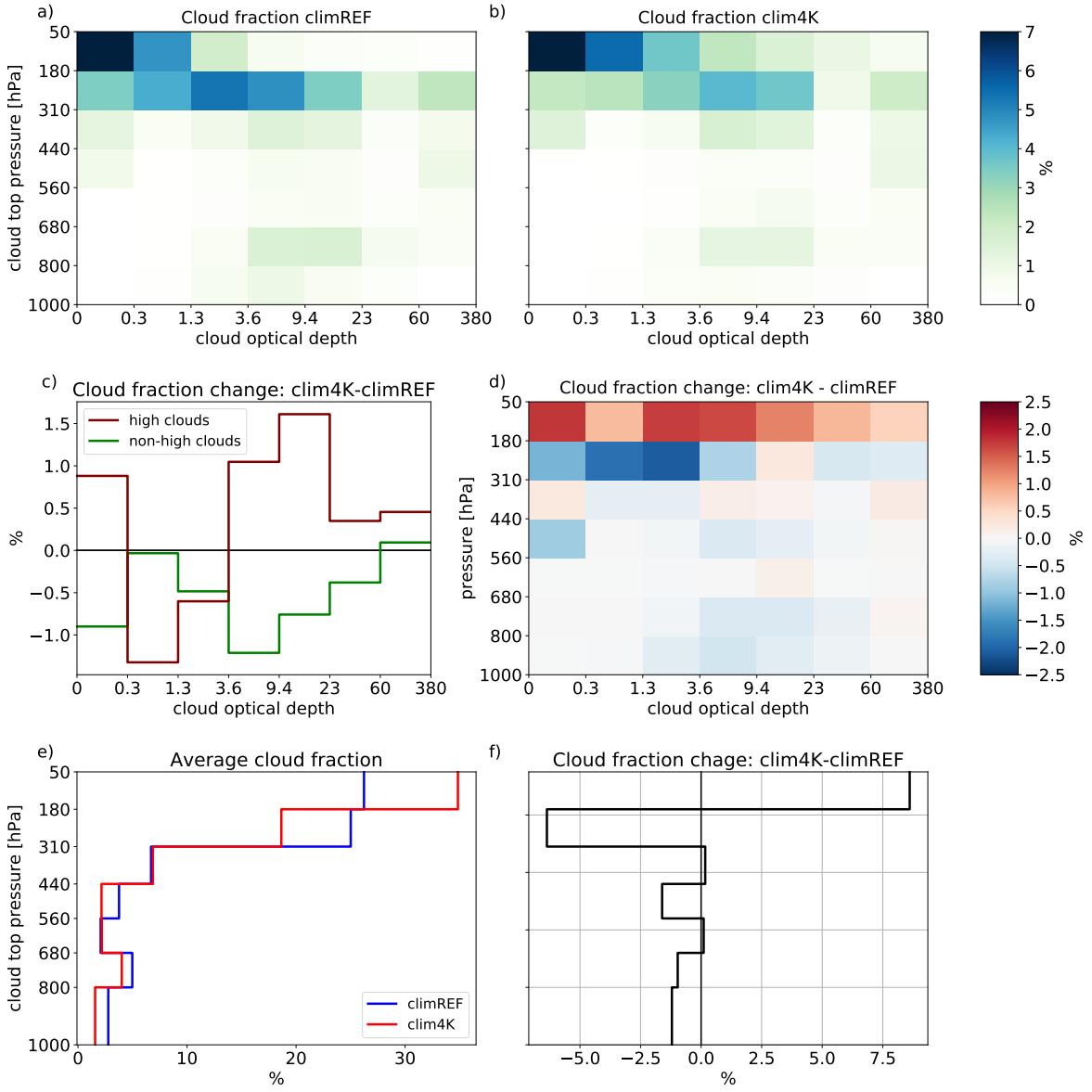

Figure S3. ISCCP cloud fraction histograms for (a) climREF, (b) clim4K simulations, and their anomaly (d). c) shows the changes in high and non-high cloud fraction as a function of cloud optical depth, averaged along cloud top pressure axis. Panel e) shows the changes in cloud fraction binned by cloud top pressure and averaged along optical depths. f) shows the respective cloud fraction anomalies.

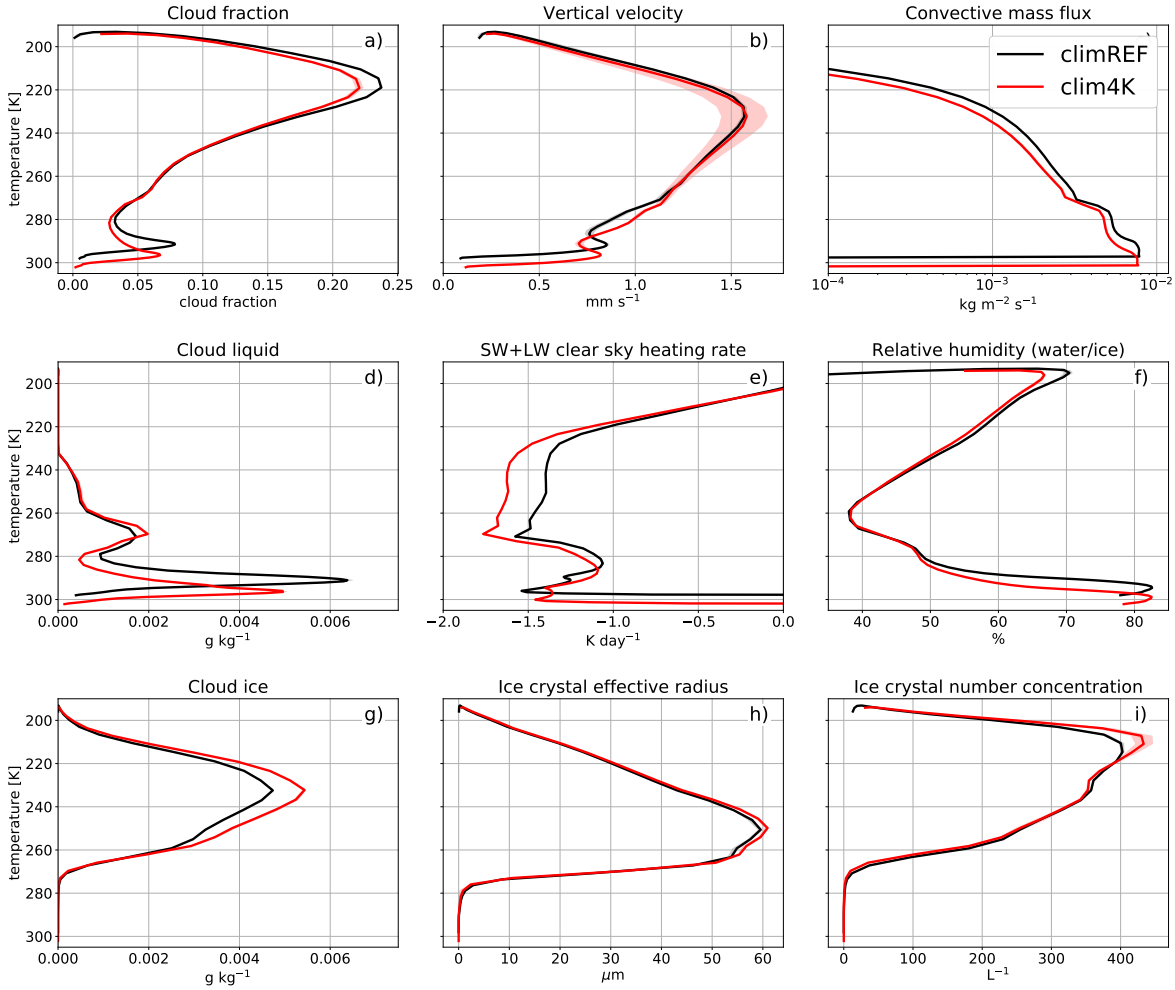

Figure S4. (a) Cloud fraction, (b) vertical velocity, (c) convective mass flux from the convective parameterization, (d) cloud liquid, (e) clear sky heating rates, (f) relative humidity with respect to water (for T>273 K), ice (for T<253 K), or a mixture between the two (for 273>T>253 K), (g) cloud ice, (h) in-cloud ice crystal effective radius, and (i) in-cloud ice crystal number concentration averaged for all gridpoints between 20°S and 20°N. The quantities are plotted as a function of temperature between the surface and approximately the tropopause level. Shaded areas cover the space between all 3 annually averaged values for each of the simulations.